Ab initio calculations of hydrogen adsorption on (100) surfaces of palladium and rhodium

S. Wilke
Fritz-Haber-Institut der Max-Planck-Gesellschaft, Faradayweg 4-6, D-14195 Berlin, Dahlem, Germany

D. Hennig and R. Löber
Humboldt-Universität zu Berlin, Fachbereich Physik, Unter den Linden 6, D-10099 Berlin, Germany
(Received 31 January 1994)

We report an all-electron density-functional-theory study of the interaction of hydrogen with Pd(100) and Rh(100) surfaces. We use the local-density approximation for the exchange-correlation energy functional and the full-potential linear-muffin-tin-orbital method. Various coverages, between $\Theta = 0.25$ and $\Theta = 2$ are considered. In particular, we discuss the adsorption energies, stable adsorption sites, adsorption-induced surface relaxations, and the work-function changes. The results show that for coverages $\Theta \leq 1$ at Pd(100) the fourfold hollow site is energetically favorable. For higher coverages it is predicted that the additional hydrogen goes subsurface. The work function is found to increase with coverage up to $\Theta = 1$ and for higher coverages (i.e., when the subsurface sites get occupied) it remains roughly at the $\Theta = 1$ level. Hydrogen adsorption at Rh(100) is found to be very similar to Pd(100) up to $\Theta = 1$. The results are compared to available experimental data as well as to other calculations.

I. INTRODUCTION

The dissociation of H_2 on transition metal surfaces represents one important step relevant for many catalytic reactions. At the same time, hydrogen adsorbed on palladium and rhodium is a prototype system of adsorbate-metal interaction. Nevertheless, a detailed understanding of the adatom geometries, their coverage dependence, and of the adsorbate-induced electronic structure does not yet exist.[1]

Experimental studies of hydrogen adsorption at Pd(100) and Rh(100) have been performed using thermal desorption spectroscopy,[2–4] work-function measurements,[2,3] low-energy electron diffraction (LEED),[3,5] electron energy-loss spectroscopy (EELS),[6,7] transmission channeling,[8] and He scattering.[9]

Hydrogen is known to adsorb dissociatively at the Pd(100) surface.[3] The adsorption energy, e.g., the energy gain per hydrogen atom by the adsorption of a hydrogen molecule on the surface, is $E_{\mathrm{ad}} = 0.53$ eV.[3] It exceeds the energy of dissolution of hydrogen in bulk palladium (0.1–0.2 eV depending on hydrogen concentration[10]) and hydrogen first occupies sites at the surface before appreciable amounts penetrate into the bulk.

Two main regimes are distinguished in the measured coverage dependence of the isosteric heat of adsorption and of the work function.[3] In the case $\Theta \lesssim 1$ the heat of adsorption is nearly independent of coverage and the work function increases linearly with coverage. The LEED experiments show two ordered phases of adsorbed hydrogen, a $c(2 \times 2)$ and the (1×1) structure.[3] In this regime the experimental data[3,6–9] are compatible with a successive occupation of surface hollow sites by hydrogen up to coverage $\Theta = 1$ where all hollow sites are filled. The occupation of the fourfold coordinated hollow sites is also consistent with the general observation that hydrogen at transition metal surfaces tends to occupy sites with the largest coordination number first.[1] Behm *et al.*[3] found that at low substrate temperatures it is possible to adsorb more than one monolayer of hydrogen in the surface region with a saturation coverage $\Theta_{\mathrm{sat}} = 1.35$ at $T = 100$ K. In the second regime with $\Theta > 1$ the isosteric heat of adsorption strongly decreases with coverage. The work function further increases linearly with coverage but the slope is larger than for coverages $\Theta < 1$. The strong decrease of E_{ad} and the increase of the work function for $\Theta > 1$ have been attributed[3,11] to the occupation of a second adsorption site at the surface (e.g., bridge or on top) in addition to the surface hollow site or to a reordering of the adlayer into islands of bridge-bonded hydrogen as found, e.g., for hydrogen on W(100).[12] Electron energy-loss experiments[6] showed for all hydrogen adsorption doses and temperatures only one single peak attributed to hydrogen in surface hollow sites and, thus, excluded the presence of a second adsorption state at the surface. Similar, He-scattering[9] experiments found no indication of the occupation of a second surface adsorption site above $\Theta = 1$. Transmission channeling experiments[8] excluded the occupation of bridge sites. A further, obvious explanation of the second adsorption state is the occupation of sites just below the surface. The presence of hydrogen at subsurface sites has been observed at the Pd(111) and Pd(110) surfaces.[13–16] In the case of hydrogen at Pd(111) no saturation of the hydrogen adsorption has been found for temperatures around 90–115 K (Ref. 13) whereas the adsorption saturates at the Pd(110) surface if all subsurface positions between the top and the first subsurface layer are filled with hydrogen.[15] A different explanation has been given

by Burke and Madix[17] who argued, in line with a possible explanation of the EELS (Ref. 6) and He-scattering experiments,[9] that the saturation coverage of hydrogen at the Pd(100) surface is $\Theta = 1$. The second adsorption state arises from hydrogen desorbing from the back side of the sample that exhibits a larger impurity concentration lowering the hydrogen adsorption energy. There are no systematical experimental or theoretical studies of subsurface hydrogen at Pd(100) and up to now, the adsorption geometry for hydrogen at Pd(100) in the second regime of Ref. 3 has not been identified.

Rhodium and palladium are neighbors in the Periodic Table of elements and the similar chemical and electronic properties reflect also in the adsorption of hydrogen at Pd(100) and Rh(100). The hydrogen atoms occupy surface hollow sites also at Rh(100). The heat of adsorption is 0.56 eV and, similar as at Pd(100), it is independent of coverage.[5,7] In contrast to Pd(100) hydrogen coverages exceeding $\Theta = 1$ have not been observed. The main and technologically important difference between both systems is the capability of palladium to form a stable concentrated hydride under normal pressure conditions whereas dissolved hydrogen in Rh is unstable against the disintegration into H_2 and pure Rh.[18]

Previous *ab initio* calculations for the Pd(100):H system[19,20] focused on the hollow, bridge, and on-top position of hydrogen and considered only the maximal possible occupation of these sites. The electronic structure of hydrogen at subsurface positions has been studied for Pd(111) (Ref. 21) but no total energies were calculated. There are no systematic studies of hydrogen adsorption at Pd(100) including subsurface sites and different coverages. The adsorption of hydrogen on Rh(100) has been studied in more detail,[22–25] but there is no comparative study of hydrogen adsorption at the Pd(100) and Rh(100) surface based on the same calculation procedure.

In this paper, we report a theoretical study of hydrogen adsorption on the Pd(100) and Rh(100) surfaces based on *ab initio* total-energy calculations using the full-potential linear muffin-tin-orbital (FP-LMTO) method.[26,27] Some of our results have been published elsewhere.[28,29] We explicitly consider adsorption geometries including subsurface and bulk sites in addition to hydrogen adsorption at different high-symmetry surface sites with various coverages. The equilibrium geometry and adsorption energy as well as the coverage dependence of the work function are calculated, as they may be compared to experimental results. In order to learn about the chemical trends in hydrogen adsorption the study was extended to hydrogen adsorption on Rh(100) surfaces.

II. METHOD

The all-electron full-potential LMTO method[26] has been previously successfully applied to bulk transition metals and the calculation of surface energies, top–layer relaxations and work functions of clean 4-*d* transition metal surfaces.[27] For the present study the metal substrate is modeled by seven layers separated by a 17 Å thick vacuum region. The hydrogen atoms are adsorbed on both sides of the metal slab. In order to describe the charge density spilled out from the surface into the vacuum region correctly, the LMTO basis has to be extended by additional orbitals centered in the vacuum region. This has been done by covering the surface with two layers of "empty" muffin-tin spheres and centering LMTO orbitals up to momentum $l = 6$ at these spheres. An adequate dense packing was achieved by placing within each of those layers empty spheres at the fcc-lattice sites (with radius 2.53 a.u.) and at the octahedral interstitial positions (with radius 1.02 a.u.). The LMTO basis set is constructed from envelopes of Hankel functions of a given angular momentum and with imaginary wave vectors centered at the individual atoms in the unit cell. At the muffin-tin spheres the Hankel functions are matched smoothly to the solution of the Schrödinger equation inside the muffin-tin sphere at a given energy and to its energy derivative. We used a basis set consisting of *s*, *p*, and *d* functions centered on every metal atom. Envelopes of Hankel functions with three different imaginary k vectors of $\sqrt{-0.7\ \mathrm{Ry}}$, $\sqrt{-1.0\ \mathrm{Ry}}$, and $\sqrt{-2.3\ \mathrm{Ry}}$ have been used, i.e., the basis has a total of 27 functions per metal atom. At the hydrogen atom *s* and *p* functions with the same wave vectors are used. The metal 4*p* states have been treated as semicore states, i.e., their contribution to the total energy has been determined in a separate band-structure calculation within the subspace of these orbitals. The calculations were done nonrelativistically solving the Kohn-Sham equations within the local-density approximation using the Ceperly-Alder parametrization[30] of the exchange-correlation potential.

The basis set of localized orbitals within the FP-LMTO method offers the possibility of calculating the density of states (DOS) projected to particular orbitals of the atoms forming up the unit cell and to perform a Mulliken analysis[31] of orbital occupation and interatomic interaction. One should have in mind that the assignment of the total charge to given orbitals as well as the projected DOS depend on the chosen basis set and is by far not unique. In the case that the same projection is used for all studied symmetries, as in our case, the concept of projected DOS is a useful tool to interpret the changes in the electronic structure and to map the result to simple chemical models.[32,33]

The adsorption geometry has been optimized within a two-parameter space consisting of the hydrogen adsorption height h_0 measured from the center of the topmost substrate layer and of the first metal-metal interlayer distance d_{12}. Usually, 3×3 energy points have been calculated and the energy minimum has been found by interpolating the values inside this area of parameter space. For hydrogen in interstitial subsurface position the parameter space comprised the distances to the two nearest metal layers d_{12} and d_{23}.

From the total energies per unit cell of the clean E_M^{tot} and hydrogen covered $E_{M:\mathrm{H}}^{\mathrm{tot}}(\Theta)$ slabs (M=Pd,Rh) the binding and adsorption energy per hydrogen atom were calculated. The *binding energy* is defined as the energy per hydrogen atom gained by adsorption of hydrogen atoms[1] up to coverage Θ

$$E_b(\Theta) = -\frac{1}{N_{\mathrm{H}}}[E_{M:\mathrm{H}}^{\mathrm{tot}}(\Theta) - E_M^{\mathrm{tot}} - N_{\mathrm{H}}E_{\mathrm{H}}^{\mathrm{tot}}]. \quad (1)$$

Here, Θ denotes the coverage defined as the ratio of the number of adsorbed hydrogen atoms (N_{H}) to the number of substrate atoms in a (100) layer. Note that we used the sign convention that a gain in energy has a positive sign. The *adsorption energy* is the energy per hydrogen atom gained by adsorption of hydrogen molecules up to coverage Θ

$$E_{\mathrm{ad}}(\Theta) = -\frac{1}{N_{\mathrm{H}}}\left[E^{\mathrm{tot}}_{M:\mathrm{H}}(\Theta) - E^{\mathrm{tot}}_{M} - \frac{N_{\mathrm{H}}}{2}E^{\mathrm{tot}}_{\mathrm{H_2}}\right]. \qquad (2)$$

The energies E_{ad} and E_b differ by the binding energy of the hydrogen molecule. The adsorption and binding energies defined above refer to the total energy gained in forming the adlayer from molecules (atoms) in the gas phase; they are integral quantities. The corresponding differential adsorption energy, on the other hand, gives the energy gain per hydrogen atom if an additional hydrogen molecule is adsorbed at a surface which is already covered with hydrogen with coverage Θ. It differs by RT from the isosteric heat of adsorption[1,34] that has been measured for the Pd(100):H system for coverages up to $\Theta = 1.3$.[3] The differential adsorption energy $\tilde{E}_{\mathrm{ad}}$ defined as the derivative of the adsorption energy with respect to the number of adatoms may be rewritten using the definition of the adsorption energy Eq. (2)

$$\tilde{E}_{\mathrm{ad}}(\Theta) = E_{\mathrm{ad}}(\Theta) - \Theta\frac{\partial E_{\mathrm{ad}}(\Theta)}{\partial\Theta}. \qquad (3)$$

In order to calculate $\tilde{E}_{\mathrm{ad}}$ the derivative in Eq. (3) is replaced by corresponding energy differences at two difference coverages. As seen from Eq. (3) the differential and integral adsorption energy are equal if the adsorption energy per hydrogen atom is independent of coverage and, hence, there are no interactions between adatoms. The differential adsorption energy is important in determining the stability of an adlayer against desorption of adatoms at T=0 K. If it becomes negative (in our sign convention) at some coverage, i. e., energy is gained if two hydrogen atoms recombine and desorb from the surface, the adlayer is unstable. In this case it disintegrates into an adlayer with a lower coverage and hydrogen molecules in the gas phase.

In order to evaluate the binding and adsorption energies [see Eq. (1) and (2)] one needs the total energies of H and H_2. We use the value $E^{\mathrm{tot}}_{\mathrm{H}} = 13.606$ eV and add the experimental binding energy of the H_2 molecule [4.75 eV (Ref. 35)] to $E^{\mathrm{tot}}_{\mathrm{H_2}} = 31.962$ eV in order to avoid the larger errors of the LDA if applied to atoms and molecules. We emphasize, that this choice of the reference system affects only the absolute values of the adsorption and binding energies; energy differences between different adsorption geometries are not influenced.

Several of our results for binding energies and adsorption heights may be compared to those obtained by previous *ab initio* calculations of hydrogen adsorption on palladium[20] and rhodium.[22,24,25] The results together with our calculation are summarized in Table I. Tománek *et al.*[20] have calculated the binding energy and adsorption height of hydrogen on Pd(100) at the hollow ($\Theta = 1$), bridge ($\Theta = 2$), and on-top position ($\Theta = 1$) applying the pseudopotential method and using a Gaussian-orbital basis set. Their findings of an energy difference between the hollow and the bridge site agrees within 50 meV with our results. For the on-top site the energy differences calculated in Ref. 20 are larger but the trend is reproduced. At the on-top site the accurate description of the electron density in the vacuum region is not without problems because the packing of empty spheres becomes less dense for short H-Pd distances. Hamann and Feibelman[22] and Feibelman[24,25] studied the Rh(100):H system. In Ref. 22 the full-potential linear augmented-plane wave method (FLAPW) is applied to hydrogen overlayers with coverage $\Theta = 1$ on Rh(100). Feibelman[24,25] uses a matrix-Green-function method to calculate the binding energy and adsorption geometry of single hydrogen atoms. A comparison of these results with the values obtained within the FP-LMTO method (see Table I) shows a very good agreement also for the absolute values of the adsorption energy. The differences are expected to be mainly due to the different degree of relaxation that has

TABLE I. Comparison of calculated binding energies and adsorption heights to other theoretical calculation and to the experiment.

Site	This paper		FLAPW		Pseudopotential		Exp.	
	E_b [eV]	h_0 Å	E_b [eV]	h_0 Å	E_b [eV]	h_0 Å	E_b [eV]	h_0 Å
Pd(100) hollow	2.83	0.11			2.92 [a]	0.24[a]	2.91[b]	<0.3[c]
Pd(100) bridge ($\Theta = 2$)	2.36	1.04			2.50[a]	1.00[a]		
Pd(100) on-top	2.20				1.86[a]	1.56[a]		
Rh(100) hollow	2.78	0.38	2.67[d]	0.58[d]	2.76[e]	0.65[e]	2.74[f]	
Rh(100) bridge	2.62	1.15	2.50[d]	1.19[d]	2.64[e]	1.12[e]		

[a]Reference 20.
[b]Reference 3.
[c]Reference 8.
[d]Reference 22.
[e]References 24 and 25.
[f]Reference 7.

been applied. We conclude, that the FP-LMTO method is applicable also to the study of hydrogen adsorption.

III. RESULTS

A. Bulk Pd and the Pd(100) surface

The properties of bulk Pd and Pd surfaces have been calculated recently[27] using the FP-LMTO method and we quote here only those results that are relevant to our discussion below.

The calculated lattice constant of fcc Pd is 3.91 Å in good agreement with the experimental value 3.89 Å.[36] The clean Pd(100) surface shows a slight inward relaxation of the topmost Pd layer of -0.6% of the bulk interlayer distance d_0 and has a calculated work function of 5.3 eV (Ref. 27) [exp. 5.22 eV (Ref. 37)]. In order to illustrate the changes of the electronic properties when going from the bulk Pd to the surface we show in Fig. 1(a) the density of states projected on the s,p orbitals (dashed lines) and d orbitals of the bulk and surface Pd atoms. The lower coordination number of surface Pd atoms leads to a reduction of the d–band width and an upward shift of the center of the d band[27] at the surface Pd atoms. At the surface about 0.2 electrons per atom spill out from surface Pd orbitals into the vacuum region and the number of holes in the surface Pd d band is increased to $0.7e$ (see also Ref. 33).

A rough estimate of the hydrogen adsorption positions may be obtained from the charge density distribution at the clean metal surface. The study of hydrogen embedded into jellium[38] has shown that the adsorption energy depends sensitively on the charge density with an optimal value at about 0.01 bohr^{-3}. If the effective medium picture is correct this optimal charge density value should be compared to the charge density averaged over the hydrogen atom size at a given adsorption site at the real surface. Figure 1(b) shows the charge density at the Pd(100) surface at a density scale around the optimum embedding charge density. The figure shows the surface hollow (circle) and subsurface (O_h) (diamond) adsorption sites divided by regions of large charge density around the palladium atoms. At the surface hollow site the optimum charge density is found just above the center of the topmost substrate layer. Actually, we found in agreement with Ref. 39 that the calculated hydrogen adsorption position corresponds to a density larger than the optimal density found from the jellium model. Around the octahedral subsurface (O_h) sites the charge density is larger than the optimal density and a decrease of the adsorption energy at these sites in comparison to surface sites is expected. Differences to the effective medium theory are expected due to the strong covalent bonds between H and Pd, but the estimate reproduces the calculated trends in the adsorption positions correctly.

B. Pd(100):H for coverage $\Theta \leq 1$

In this section, we consider hydrogen coverage range up to $\Theta = 1$. Within this range all experimental studies

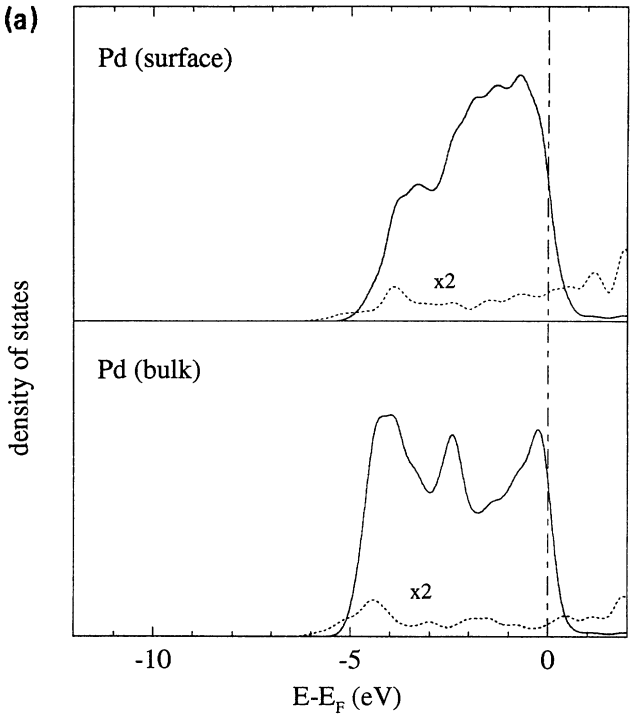

FIG. 1. Layer and symmetry resolved DOS (a) and charge density distribution (b) at the clean Pd(100) surface. (a) DOS projected to the d (solid line) and s,p functions (dashed line) of the surface (upper panel) and bulk (lower panel) Pd atoms. (b) Charge density for a cut plane perpendicular to the surface and along the ⟨100⟩ direction. The scale is given in 10^{-2} bohr^{-3}.

agree that the adsorption process occurs via the subsequent occupation of the surface hollow sites up to their maximal occupation at $\Theta = 1$. We will discuss the energetic differences between different high-symmetry adsorption sites and the coverage dependence of the adsorption energy.

Table II summarizes at $\Theta = 1$ the calculated adsorption and binding energies, the equilibrium geometry, and the change of the work function in comparison to the clean Pd(100) surface for hydrogen at surface sites as well as for hydrogen placed at subsurface interstitial positions with octahedral (O_h) and tetrahedral (T_d) symmetry.

As expected, the surface hollow position is found to be the most stable adsorption site. The calculated adsorption energy using the value 31.962 eV for the total energy of the H_2 molecule (see Sec. II) is 0.47 eV. It is in good agreement with the experimental value of 0.53 eV.[3] The adsorption height measured from the surface metal centers is only $h_0 = 0.11$ Å and the hydrogen atoms are well embedded inside the surface. In response to the hydrogen adsorption the inward relaxation of the topmost Pd layer found at the free surface is removed and we obtained a noticeable outward relaxation of the topmost palladium layer of $\Delta d_{12} = +5.2\%\ d_0$. The increase of the first interlayer spacing d_{12} is found to scale linearly with hydrogen coverage. The large outward relaxation reflects the decohesion of metal-metal bonds in the presence of hydrogen, an effect closely related to the large increase of atomic volume and the loss of mechanical stability found in concentrated bulk palladium hydride.[12,40] Experimentally, an outward relaxation was expected from the analysis of the *I-V* curves of the LEED spectra of hydrogen covered Pd(100).[3,11]. Most interesting, a study of the multilayer relaxation of clean Pd(100) using LEED (Ref. 41) revealed an anomalous outward relaxation of the topmost metal layer of 3% d_0. The authors of Ref. 41 suggested two possible mechanisms: the presence of interstitial hydrogen in the surface region or the presence of magnetic moments in the surface layers of Pd. Our results are consistent with the first mechanism. Both, hydrogen at the surface, as well as in interstitial positions just below the surface induce an outward relaxation of the topmost Pd layer that would explain the measured value of the increase of the first interlayer spacing. The position of the hydrogen atom relative to the surface has been measured by transmission channeling[8] to $\Delta z = 0.30 \pm 0.05$ Å. This value has to be compared to our adsorption height h_0 adding the outward relaxation of the topmost metal layer. We obtain $\Delta z = 0.2$ Å in agreement with the measured value. The hydrogen adsorption energy as well as the adsorption height depend on the state of relaxation of metal substrate. If we assume that the metal substrate has not yet relaxed and calculate the hydrogen adsorption on the Pd(100) substrate with the first metal-metal interlayer spacing fixed to its value at the clean surface ($\Delta d_{12} = -0.6\%\ d_0$) the adsorption energy is at $\Theta = 1$ by 30 meV per hydrogen atom lower than at the fully relaxed surface and the adsorption height is increased to $h_0 = 0.16$ Å.

The difference of the adsorption energy between the surface hollow site and other adsorption positions is significant, namely at least 0.28 eV at $\Theta = 1$. This stabilizes the surface hollow sites against geometries involving other adsorption sites even at higher temperatures. There are two interesting trends in the adsorption energy if different adsorption sites are compared. First, the adsorption energy decreases with decreasing number of nearest-neighbor Pd atoms. At the surface the fourfold coordinated hollow site has a larger adsorption energy than the twofold coordinated bridge site, and that again has a higher energy than the on-top site. The same trend is followed for the octahedral and tetrahedral subsurface sites. Second, a large decrease in adsorption energy is found between surface and subsurface sites. We calculated the artificial geometry of a layer of hydrogen in bulk Pd and found small differences between hydrogen placed at subsurface (O_h) sites and hydrogen at interstitial (O_h) sites deeper in the bulk.

As expected from the large dissolution energies of hydrogen in palladium the adsorption energy of hydrogen in subsurface (O_h) sites is large. It compares to that of the surface bridge position. In line with the volume increase by hydrogen incorporation in concentrated palladium hydride and the outward relaxation found for hydrogen adsorbed at the surface a large increase of the distance between a (100) Pd subsurface layer containing hydrogen and the neighboring (100) Pd layers is obtained (see Table II). The increase of volume per hydrogen atom (12%) is the same as obtained for bulk PdH. The energy difference between hydrogen adsorbed at the surface and in subsurface (O_h) sites is much larger for the Pd(100) surface ($\Delta E_{ad} = 0.28$ eV) than that calculated for the

TABLE II. Calculated values of the adsorption energy E_{ad}, binding energy of hydrogen E_b, adsorption height h_0, top-layer relaxation Δd_{12} and work function change $\Delta\Phi$ for H on Pd(100). For the clean surface the top-layer relaxation is −0.6 % and the work function is 5.3 eV.

Adsorption site	Coverage Θ	E_b [eV]	E_{ad} [eV]	h_0 [Å]	Δd_{12} $\%d_0$	$\Delta\Phi$ [meV]
Hollow	1	2.83	0.47	0.11	+5.2	180
Bridge	1	2.51	0.14	1.01	+3.2	390
On-top	1	2.20	−0.15	(1.56)[a]	(0)	180
Subsurface (O_h)	1	2.55	0.19		+5.2	−190
Subsurface (T_d)	1	2.31	−0.06		+10.4	−290

[a]The distances in parentheses indicate that they were not allowed to relax.

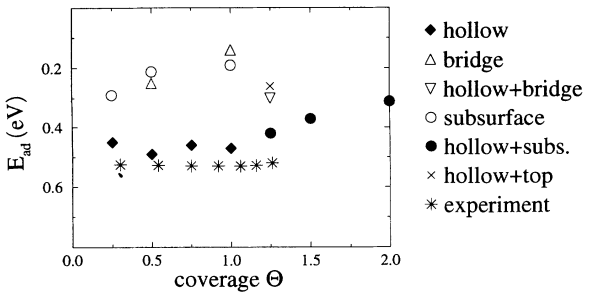

FIG. 2. Calculated coverage dependence of the adsorption energy for hydrogen adsorption on Pd(100) in various adsorption geometries denoted on the right.

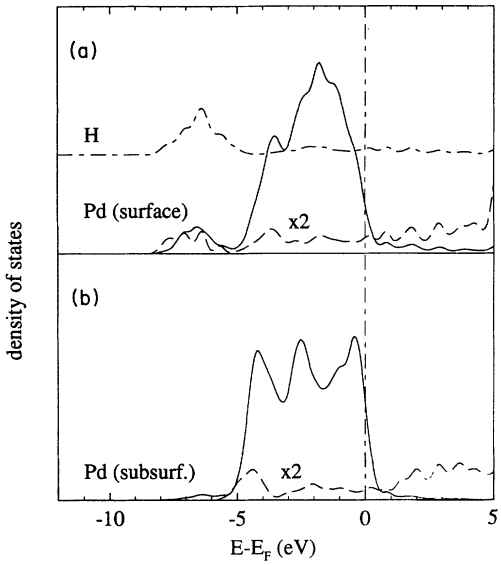

FIG. 3. Layer and symmetry resolved DOS for the Pd(100)-(1×1)-H(hollow) structure. Given are the DOS projected to hydrogen s,p functions and to the d (solid line) and s,p functions (dashed line) of the surface (upper panel) and subsurface (lower panel) Pd atoms.

Pd(111) ($\Delta E_{ad} = 0.1$ eV) surface at $\Theta = 1$. This has its origin in the different geometry of the hydrogen subsurface (O_h) position. At the (100) surface the subsurface (O_h) sites are located within a Pd metal layer and the H-Pd distance inside the layer is fixed to 1.94 Å, about 4% smaller than in PdH. At the (111) surface the subsurface (O_h) position is between two metal layers and all Pd-H bond lengths are free to relax by increasing the distance between the adjacent (111) Pd layers.

Figure 2 shows the coverage dependence of the adsorption energy for various hydrogen coverages and adsorption geometries. The results clearly confirm that for $\Theta < 1$ H_2 adsorbs dissociatively at the Pd(100) surface and the hydrogen atoms occupy the surface hollow sites. In agreement with experimental data[3] the coverage dependence of the adsorption energy is small for hydrogen adsorbing at surface hollow sites. The calculations indicate a slight maximum of the adsorption energy at $\Theta = 0.5$ which is in agreement with the experimentally observed formation of islands for coverages near $\Theta = 0.5$ (Ref. 3) and the calculated attractive interaction between hydrogen atoms in second nearest neighbor positions.[42,43]

C. Discussion of hydrogen bonding

In order to understand the trends found for the adsorption energy in the previous paragraph we analyze the hydrogen bonding at the Pd(100) surface in more detail.

If hydrogen adsorbs on palladium, characteristic changes of the electronic structure in comparison to that of the clean surface are found.[19–21,33,44–46] In Fig. 3, we show as an example the layer and orbital resolved density of states for hydrogen adsorbed at the hollow sites with coverage $\Theta = 1$. The dashed-dotted line shows the density of states at the hydrogen atom, the dashed line gives the s,p–orbital contribution and the solid line the d–orbital contribution to the density of states at the surface and subsurface Pd site. Figure 3 should be compared with the DOS at the clean surface (Fig. 1).

Most characteristic for the interaction of hydrogen with palladium is the formation of a band about 6.5 eV below the Fermi energy and situated below the band edge of pure palladium. At the same time the density of states in a region down to about −2 eV below the Fermi energy is reduced due to a shift of the d–band DOS to lower energies. The changes of the DOS introduced by the adsorbed hydrogen are confined to the layer to which the hydrogen is bound. Already in the subsurface metal layer they are well damped out as seen in Fig. 3 for the DOS projected to the subsurface layer. Similar, if hydrogen is placed to the subsurface layer the DOS at the surface remains nearly unchanged.

In Fig. 4(a) the energy scale of Fig. 3 for the surface DOS is expanded and Fig. 4(b) shows the charge density distribution for the energy range of the H-Pd bonding band at hydrogen coverage $\Theta = 1$. The charge density is plotted for a cut perpendicular to the surface down to the second subsurface metal layer. At the surface it goes along the ⟨110⟩ direction and includes three nearest neighbor hydrogen atoms.

The H-Pd bonding band arises from a strong interaction of hydrogen states with both, the surface Pd d and s,p states.[33] This band is a H-Pd bonding band as is seen from the nearly equal contribution of H s and Pd s,p orbitals to the DOS in Fig. 4(a). The reduction of states in the region below the Fermi level due the bonding of hydrogen to the surface Pd atoms at $\Theta = 1$ indicates that the possibility of Pd to form bonds with hydrogen is saturated if one hydrogen atom bonds to one surface Pd atom. This is also expected from the position of Pd in the Periodic Table just before the noble metal Ag. The density of states at the Fermi level determines the length over which perturbations of the charge density at the surface are screened. The Thomas-Fermi screening length may be estimated inserting for the relevant DOS at the Fermi level the spatial average around the given adsorption site of the charge density from states close to the Fermi level. In the case of the surface hollow and the subsurface (O_h) sites of the Pd(100) surface we found at the clean surface

a screening length of about 0.7 Å. This value is smaller than half the distance between two hollow sites (1.4 Å) at the Pd(100) surface and one expects a good screening of adsorbate-induced changes in the surface charge density[47] and a small interaction between the hydrogen atoms. The screening length is slightly increased to 0.8 Å if up to one monolayer of hydrogen is adsorbed at the Pd surface. Integrating the layer resolved DOS up to the Fermi level we obtained an excess charge at the surface in comparison to the case without hydrogen adsorption due to the screening of the hydrogen atoms. This charge is located mainly near the hydrogen proton and a total of about $1.3e$ is found in the hydrogen LMTO orbitals. The excess charge in the surface region is provided by the subsurface and bulk region as expected for metallic screening. In the case where more than one monolayer of hydrogen is adsorbed at surface positions ($\Theta > 1$) the density of states at the Fermi level projected to Pd atoms to which two hydrogen atoms are bonded strongly decreases. The screening length in those regions with local coverage $\Theta = 2$ increases to about 1.1 Å resulting in a repulsive interaction of nearest-neighbor hydrogen atoms. A similar effect is observed palladium hydride, where for hydrogen concentration exceeding ≈ 0.6 the Fermi level crosses the top of the d band and is located in the s,p band[10] with low density of states.

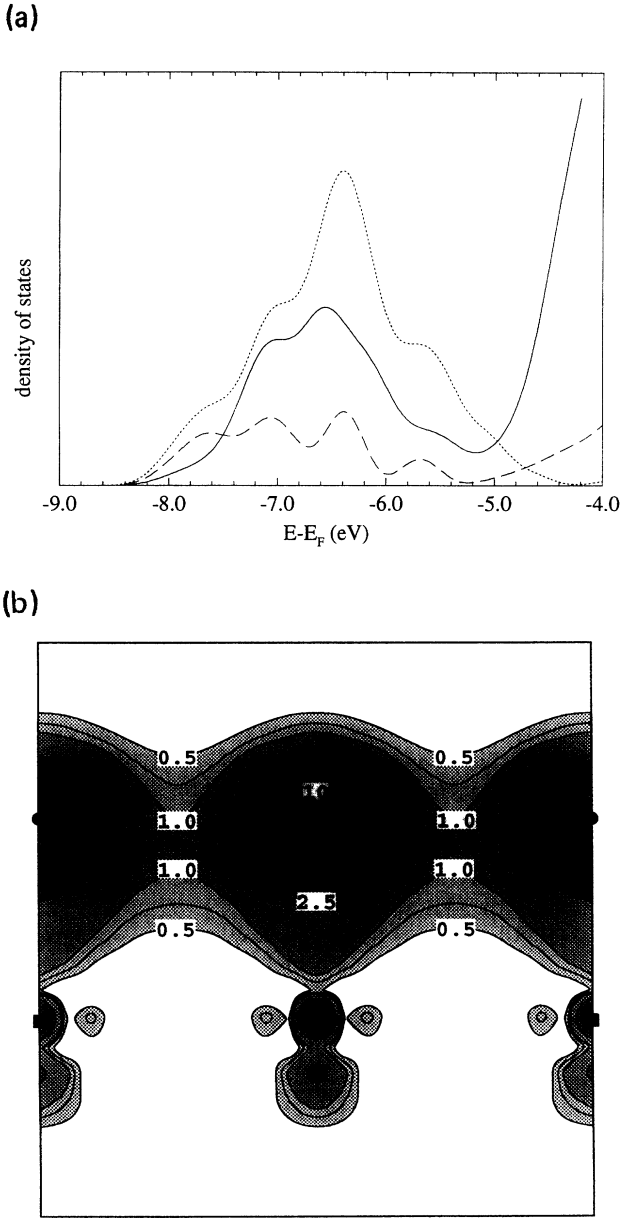

FIG. 4. Layer and symmetry resolved DOS (a) and charge density distribution (b) in the energy range of the split-off band of the Pd(100)-(1×1)-H(hollow) structure. (a) DOS projected to hydrogen s,p functions (dashed-dotted line) and to the d (solid line) and s,p functions (dashed line) of the surface Pd atoms. (b) Charge density for a cut plane perpendicular to the surface and along the ⟨110⟩ direction. The scale is given in 10^{-2} bohr^{-3}.

The different character of hydrogen bonding to Pd s,p and d orbitals is illustrated by the different spectral dependence of the s,p- and d-orbital contributions to the Pd DOS in Fig. 4(a). In correspondence with the picture of a covalent bond we found that the contribution of d functions to the H-Pd bonding band is more localized than the s,p contributions and that its center shifts to lower energies with increasing coordination number of Pd atoms but is nearly independent of hydrogen coverage. The H-Pd bonding band is in resonance with the bottom of the d band for hydrogen atoms placed at bridge sites, shifts to -6.5 eV and -7.5 eV if the hydrogen is placed into surface hollow or subsurface octahedral interstitial sites, respectively. The analysis of the overlap contributions in the Mulliken decomposition[31] of the DOS shows that the bonding of hydrogen to the d orbitals of Pd is bonding in nature. The contribution from the s,p functions, on the other hand, extends to lower energies, has a larger band width, and merges into the bulk band. In the case that the hydrogen is placed into subsurface (O_h) positions there is nearly no contribution of Pd s,p states to the H-Pd bonding band and the hydrogen bonds mainly to the Pd d states. In accordance with the increased charge density at subsurface positions [see Fig. 1(b)] in comparison to surface hollow positions and the corresponding increase of kinetic energy (see Sec. II A) we found that the interaction between hydrogen and Pd s,p states is bonding at the surface but is antibonding for hydrogen in subsurface (O_h) sites. These results confirm the possibility to interpret the hydrogen bonding to transition metals in terms of relative independent metal and covalent bonding contributions of the H-Pd bond. Both parts, however, cannot be strictly divided and the DOS in Fig. 4(a) illustrates the hybridization and overlap between both contributions.

The density plot of the H-Pd bonding band in Fig. 4(b) confirms that the bonding of hydrogen to the palladium surface at larger concentrations does not consist of individual well isolated H-Pd bonds but, opposite, the hydrogen-induced states are delocalized over the whole surface plane and form a surface band. Perpendicular to the surface the states are strongly localized as expected already from the behavior of the layer resolved DOS. The distance between the hydrogen atoms at the Pd surface

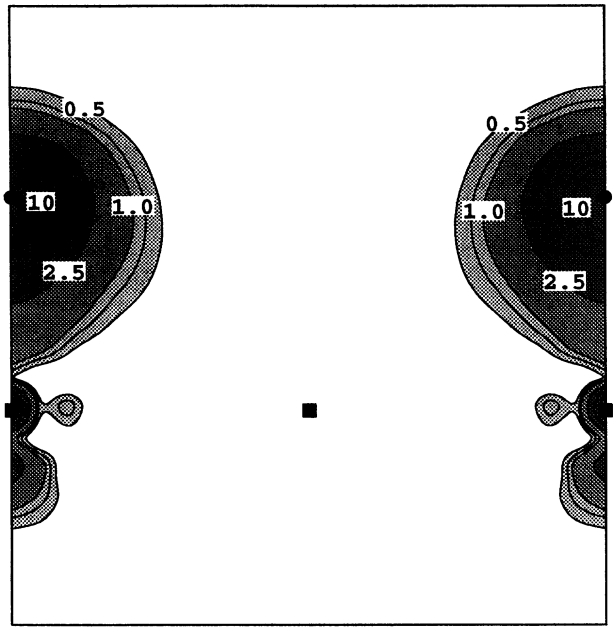

FIG. 5. Charge density distribution in the energy range of the split-off band of the Pd(100)-(2×2)-H (hollow) structure in the same cut plane as in Fig. 4.

(2.8 Å) at $\Theta = 1$, however, is too large for a direct interaction between these atoms but the strong bonding of hydrogen to surface Pd atoms mediates an indirect interaction between the hydrogen atoms.[48] The formation of a surface band was found down to coverages $\Theta = 0.5$. At $\Theta = 0.25$ the character of the low-energy H-Pd states becomes qualitatively different. In Fig. 5, we show the charge density of the H-Pd bonding states at the surface hollow sites for coverage $\Theta = 0.25$ in the same cut plane as before. The band disintegrates into individual H-Pd bonding states localized to the hydrogen and its nearest-neighbors Pd atoms. The different character of the H-Pd bond should also reflect in the coverage dependence of physical quantities, as e.g., the work function. In the case of palladium hydride those differences between low (α phase) and high concentrations of hydrogen (β phase) are also found for the energy of dissolution and the increase of atomic volume in palladium hydride PdH_x.[10,40,49,50]

D. Pd(100):H for coverage $\Theta > 1$

At coverage $\Theta = 1$ the hydrogen fully occupies the surface hollow sites, as was discussed in the preceding paragraphs. At larger coverages we consider the following three adsorption geometries for the additional hydrogen atoms. First, the additional hydrogen occupies a further adsorption site at the surface. We place hydrogen atoms into bridge and on-top position in addition to the surface hollow sites. Second, it is conceivable that islands of bridge-bonded hydrogen form with local coverage $\Theta = 2$ whereas all other hydrogen atoms occupy surface hollow sites. In this case a part of the hydrogen atoms that occupy at $\Theta = 1$ hollow sites have to convert to the bridge site. In the third geometry the additional hydrogen goes subsurface. We consider the case where in addition to the surface hollow sites the octahedral positions just below the surface become occupied.

Table III summarizes the adsorption energy at coverage $\Theta = 1.25$ for the different adsorption geometries. The differential adsorption energy $\tilde{E}_{ad}$ [see Eq. (3)] has been estimated from the adsorption energies at $\Theta = 1.25$ and $\Theta = 1$.

The results show that at coverages $\Theta > 1$ the energetically most favorable site for the additionally adsorbed hydrogen atoms is subsurface. The adsorption energy $\tilde{E}_{ad}$ has nearly the same value as the adsorption energy of a $\Theta = 0.25$ occupation of subsurface sites (see Fig. 2) indicating a small interaction between hydrogen atoms in the surface hollow and the subsurface (O_h) sites.

In the case that all hollow and an additional second site at the surface are occupied, a large repulsive H-H interaction contribution to the adsorption energy of about 0.5 eV is found. As a consequence, the differential adsorption energy is negative and those configurations become unstable against desorption of the additional hydrogen as molecules. The interaction energy decreases to 0.28 eV if islands of bridge-bonded hydrogen are formed. In order to form those islands at coverages $\Theta > 1$, part of the hydrogen atoms occupying the hollow positions at $\Theta = 1$ have to convert to the bridge positions before the hydrogen is adsorbed at the remaining bridge sites. The large conversion energy [0.33 eV per hydrogen atom at the Pd(100) surface] gives an additional large negative contribution to $\tilde{E}_{ad}$ and makes the formation of islands of bridge-bonded hydrogen with local coverage $\Theta = 2$ energetically even more unfavorable. A similar conclusion has been found already in Ref. 20 where the stability of bridge hydrogen with coverage $\Theta = 2$ has been studied. From our results we conclude more generally, that all configurations where more than one hydrogen atom bonds to a palladium atom are energetically unfavorable.

The large repulsive interaction of hydrogen atoms in configurations with local coverage $\Theta = 2$, as discussed in the preceding paragraph, has its origin in the strong decrease of the density of states at the Fermi level for

TABLE III. Calculated values of the adsorption energy and the work function change compared to the clean Pd(100) surface for $\Theta = 1.25$. Given are the averaged adsorption energy E_{ad} per hydrogen atom and the adsorption energy per hydrogen atom $\tilde{E}_{ad}$ [see Eq. (3)] of the additional 0.25 monolayer (ML) hydrogen atoms adsorbing at a Pd(100) surface covered with 1 ML hydrogen at the hollow sites.

Adsorption site	E_{ad} [eV]	$\tilde{E}_{ad}$ [eV]
Hollow ($\Theta = 1$)+ on-top ($\Theta = 0.25$)	0.26	−0.59
Hollow ($\Theta = 1$) + bridge ($\Theta = 0.25$)	0.30	−0.39
Hollow ($\Theta = 0.75$) + Double-bridge ($\Theta = 0.5$)	0.35	−0.47
Hollow ($\Theta = 1$) + subsurface ($\Theta = 0.25$)	0.42	0.22

those configurations. Charge density plots show a large enhancement of the charge density in the region between nearest-neighbor H atoms. On the other hand, if the additional hydrogen goes subsurface the surface and the subsurface palladium layers participate in the bonding to hydrogen. The hydrogen atoms in both layers are even decoupled due to the increased interlayer distance d_{12} between the surface and the subsurface layer. The charge density distribution within each of these layers as well as the local density of states are not strongly influenced by the presence of the other hydrogenated layer.

The calculated coverage dependence of the averaged adsorption energy for hydrogen adsorption on Pd(100) is shown in Fig. 2 by filled symbols. In agreement with the experiment we found a decrease of the adsorption energy E_{ad} if more than one monolayer of hydrogen is adsorbed and the additional hydrogen starts to occupy subsurface sites. At larger occupation of the subsurface (O_h) sites the (integral) adsorption energy follows closely the weighted average between the adsorption energies of separately fully occupied subsurface (O_h) and hollow positions. The differential adsorption energy is expected to saturate near the value of the adsorption energy of hydrogen at subsurface (O_h) sites. It would be interesting to extend the experiments to higher saturation coverages to prove this conclusion.

In order to explain the experimentally observed saturation coverage of hydrogen on Pd(100) one should note that we found a saturation of hydrogen adsorption *on the surface* at a coverage $\Theta = 1$. In the case where for coverages $\Theta > 1$ the additional hydrogen occupies subsurface (O_h) sites, no decrease of the adsorption energy to negative values is observed (see Fig. 2) limiting the occupation of those sites. A possible explanation of a hydrogen saturation coverage $\Theta > 1$ was given in Ref. 17 where the authors argued that the hydrogen may originate from the back of the crystal, with impurities causing the downward shift of the desorption temperature. A different explanation, consistent with our calculation, is the formation of a concentration profile of hydrogen due to the diffusion of hydrogen from the surface into the bulk of the material. The low temperature desorption peak as well as a change in the work function originate exclusively from hydrogen placed in a region close to the surface. Dissolved hydrogen is known to give rise to a separate broad peak in desorption experiments at temperatures larger than about 550 K.[3] The hydrogen concentration profile at a given temperature will be mainly determined by the interplay of diffusion from the surface to the subsurface at the one side and the diffusion away from the subsurface into the bulk on the other. The observed saturation coverage reflects the concentration profile in a region close to the surface. This is also in agreement with the experimentally observed increase of the saturation coverage with decreasing temperature.[3,11]

E. The work function

The change of the work function in comparison to the clean Pd(100) surface has been measured for hydrogen adsorption on Pd(100) for coverages $0 < \Theta < 1.3$.[3] In Fig. 6, the theoretical results of the coverage dependence of the work function are shown together with the experimental data of Ref. 3. The calculations are performed for ordered layers of hydrogen adsorbates. According to the calculated equilibrium geometries, hollow sites are occupied up to coverage $\Theta = 1$. At coverages $\Theta > 1$ hydrogen is placed at subsurface (O_h) positions in addition to the fully occupied surface hollow sites. The change of the work function due to hydrogen adsorption at other adsorption sites at $\Theta = 1$ is given in Table II.

In correspondence with the different adsorption geometries for $\Theta < 1$ and $\Theta > 1$ two trends are identified in the theoretically calculated dependence of the work function on coverage. The work function increases with increasing hydrogen coverage up to $\Theta = 1$ and reproduces the trend found in the experiment. The absolute values of the calculated work function for ordered structure are larger than in the experiment. The increase of the work function has its origin in the accumulation of screening charge in the surface region as discussed above. Furthermore, a charge density difference plot between the hydrogen covered surface and a superposition of the charge density of the clean surface and neutral atomic hydrogen shows a local redistribution of charge close to the surface Pd atoms towards the on-top region. The changes in the work function are found to depend strongly on the adsorption height h_0 and the first interlayer distance d_{12}. In the case of the Pd(100)-(1×1)-H phase we obtained $\partial\Phi/\partial h_0 \approx 0.6$ eV/Å and $\partial\Phi/\partial d_{12} \approx 0.2$ eV/Å.

At coverages $\Theta > 1$ the work function varies only slightly with coverage and saturates for $\Theta = 2$ at a value near or just below the value found at $\Theta = 1$ for fully occupied hollow sites. This behavior is in agreement with the expectation that the work function is determined mainly by hydrogen at the surface. Hydrogen in a subsurface position tends to decrease the work function. This decrease is much more pronounced if hydrogen is placed

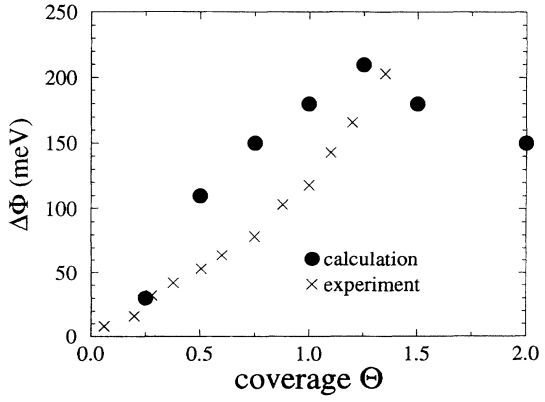

FIG. 6. Calculated coverage dependence of the work-function change (filled circles) and experimental results (×) from Ref. 3. The work functions were calculated for ordered structures where the hydrogen occupies surface hollow sites up to $\Theta = 1$ followed by an occupation of subsurface (O_h) sites by the additional hydrogen atoms.

exclusively into subsurface (O_h) positions. In this case the work function decreases by about 190 meV (see Table II) below the value of the clean Pd(100) surface if all interstitial (O_h) sites in the subsurface layer are occupied. In all geometries where for $\Theta > 1$ all hydrogen was assumed to adsorb on the surface, a strong decrease of the work function below the value of the clean surface has been observed. This trend is in contrast to the increase of work function found experimentally[3] and confirms the conclusion that the additional hydrogen for $\Theta > 1$ is not placed at the surface.

It is interesting to note that we obtained in deviation from the above trends a slight increase of the work function at coverage $\Theta = 1.25$. No increase of the work function has been obtained if hydrogen has been placed exclusively into subsurface positions. The deviations found at $\Theta = 1.25$ and also for small occupation of hollow sites at $\Theta = 0.25$ falls together with the formation localized H-Pd bonding states at small hydrogen concentration in a Pd(100) layer as discussed in Sec. III C. A possible explanation for this unexpected result, that the occupation of subsurface sites may increase the work function, is as follows. Close to the hydrogen atoms an increase of charge density due to the screening of the proton is found. If exclusively subsurface sites are occupied part of the screening charge is provided also by the surface atoms and this charge flow results in a decrease of the work function. In the case that the hollow sites are occupied the screening charge comes only from the bulk material and gives rise to an increase of charge in the surface region and of the work function. At larger hydrogen occupations in the subsurface layer the charge density in the surface region becomes too large and the repulsive interaction between hydrogen atoms at the surface and in the subsurface leads to a charge reduction of charge at the surface. An indication of this mechanism is obtained from the Mulliken analysis. At $\Theta = 1.5$ a reduction of charge at the surface Pd atoms is found in comparison to $\Theta = 1$ but not at $\Theta = 1.25$. Within our method the calculation of small differences in the work function in large surface units cells is not without problems and a detailed analysis of this interesting behavior is in progress.

The calculated increase of the work function at $\Theta = 1.25$ indicates that the occupation of subsurface sites with hydrogen may explain the observed increase of the work function for a restricted coverage range above $\Theta = 1$. At larger occupation of subsurface sites, however, we expect a decrease and saturation near the value at $\Theta = 1$. Further experimental data would be extremely desirable to confirm this conclusion.

F. Rh(100):H

To learn about the chemical trends in hydrogen adsorption on transition metals we compare Pd(100):H to hydrogen adsorption on Rh(100). The main difference between both transition metals is the different number of d electrons.

The calculated lattice constant of Rh is 3.81 Å, again close to the experimental value of 3.82 Å. At the clean Rh(100) surface a decrease of the first interlayer distance of -3.5% is found.[27] The larger value of the top layer relaxation in comparison to the Pd(100) surface results from stronger Rh-Rh bonds due to decreased occupation of antibonding d-d orbitals in Rh.[27] The stronger Rh-Rh bond results also in an increase of the d-band width from 5.3 eV in Pd to 6.5 eV in Rh. The density of states at the Fermi level and also the Thomas-Fermi screening length are nearly the same at Pd(100) and Rh(100) but the Fermi level is located well inside the d band of Rh. In Fig. 7, we show the charge density distribution at the Rh(100) surface at the same scale as for Pd(100) in Fig. 1(b). In the case of rhodium the regions of large charge density around the metal atoms fill a larger portion of space than in Pd. This is a consequence of the smaller lattice constant and the larger d-shell radius of rhodium in comparison to palladium. Figure 7 illustrates the outward shift of the charge density region favorable for hydrogen adsorption at the surface and the increase of charge density in the subsurface (O_h) positions in comparison to the Pd(100) surface. We expect from these trends a larger adsorption height of hydrogen in the surface hollow sites and a decrease of the energy of dissolution of hydrogen in Rh.

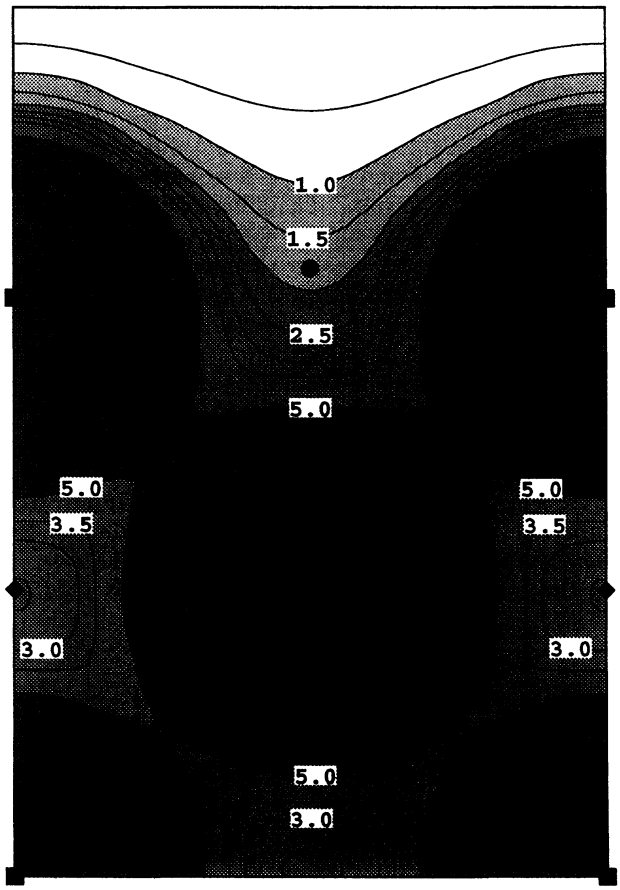

FIG. 7. Charge density distribution at the clean Rh(100) surface for the same cut plane as in Fig. 1.

We calculated the properties of a RhH compound. The lattice constant is found to be expanded by 4.8% in comparison to pure Rh. The calculated value of 4.0 Å is close to the experimental value of 4.02 Å.[18] The energy of dissolution is −0.06 eV and in agreement with experiment[18] we found that RhH is not stable against a decomposition into pure Rh and H_2 molecules. In difference to Pd no appreciable amounts of hydrogen are loaded into the bulk of Rh under normal temperature and pressure conditions.

In Table IV, we collected the calculated parameters of the equilibrium geometry, the adsorption and binding energy, and the work function change in comparison to the clean Rh(100) surface for different atomic arrangement of hydrogen at the surface and in subsurface (O_h) positions.

Hydrogen adsorption at the Rh(100) surface is very similar to that at the Pd(100) surface in contrast to the differences observed in bulk absorption. The surface hollow site is the stable adsorption site up to monolayer coverage. The adsorption energies for hydrogen on Rh (E_{ad}=0.42 eV) is only slightly smaller than for hydrogen on Pd (E_{ad}=0.47 eV). As for Pd the adsorption energy does nearly not change with concentration. We found adsorption energies of 0.39 eV and 0.38 eV for the Rh(100)-$c(2 \times 2)$-H and Rh(100)-(2×2)-H structure, respectively. As argued from the charge density distribution at the clean surface the adsorption height of hydrogen in the hollow position (h_0=0.38 Å) at Rh(100) is larger than for Pd(100) but the hydrogen remains well embedded into the surface. Hydrogen adsorption increases the first interlayer distance compared to the clean surface by about 4.8% d_0 to Δd_{12} =+1.1% d_0. The relative increase is close to the value found for Pd(100) but due to the larger inward relaxation found at the clean surface a smaller outward relaxation results. The difference of the adsorption energy between the surface hollow and bridge sites of 0.18 eV is considerably smaller than at the Pd(100) surface (0.33 eV). The occupation of subsurface (O_h) sites is energetically unfavorable as expected from the negative energy of dissolution of bulk RhH.

In order to discuss the possibility of hydrogen coverages $\Theta > 1$ we calculated the adsorption energy for two configurations at $\Theta = 2$. First we occupied one bridge site in addition to the fully occupied hollow sites and second, hydrogen was placed at all bridge positions. The occupation of subsurface (O_h) sites in addition to the hollow site is ruled out for hydrogen on Rh(100).

In the case that the hollow and the bridge sites are occupied we found a repulsive H-H interaction contribution to the adsorption energy of about 0.47 eV. It is in the same order of magnitude as found for the same configuration of hydrogen at Pd(100). A similar value has been obtained within the FLAPW method.[22] The large repulsive interaction between hydrogen atoms at the hollow and bridge sites at Pd(100) as well as at Rh(100) makes the simultaneous occupation of bridge and hollow sites energetically unfavorable.

The repulsive interaction between hydrogen atoms is reduced in islands of bridge-bonded hydrogen with local coverage $\Theta = 2$. The adsorption energy per hydrogen atom adsorbed at bridge sites is 0.21 eV at $\Theta = 2$ and only slightly smaller than for configurations where only one bridge site per unit cell is occupied. The small interaction of about 0.06 eV between hydrogen atoms in bridge positions for $\Theta = 2$ at Rh(100) is in contrast to the large repulsive interaction found for hydrogen on Pd(100). This difference is a consequence of the smaller number of electrons in the Rh d band. In contrast to hydrogen adsorption at Pd(100) the position of the Fermi level remains inside the d band for hydrogen coverages $\Theta > 1$ on the surface. At $\Theta = 2$ the value of the screening length (≈ 0.7 Å) remains smaller than half the distance between nearest-neighbor bridge atoms (1 Å). The larger number of unoccupied d states provides also a larger number of orbitals capable of bonding with hydrogen atoms.

The difference adsorption energy $\tilde{E}_{ad}$ of the double bridge configuration at Rh(100) is given by the difference between the energy required to transform a hydrogen atom from the hollow to the bridge site (0.18 eV) and the energy gain by adsorbing a second hydrogen atom at the empty bridge sites (0.18 eV). This energy difference is nearly zero at the Rh(100) surface in contrast to the large negative value at Pd(100). The energy difference is too small that we may conclude about the possibility for coverages $\Theta > 1$ on Rh(100) surfaces but the result shows that the stability of bridge-bonded hydrogen at $\Theta = 2$ is sensitive to the actual transition metal surface.

The work function of the clean Rh(100) surface was calculated to 5.25 eV in good agreement with experiment.[51] The work function increases with increasing occupation of the surface hollow sites. The work function changes at $\Theta = 0.5$ by 220 meV in agreement with the experimental value of 200 meV.[51] The increase is larger compared to hydrogen on Pd(100) in correspondence to the larger adsorption height. At monolayer coverage a work func-

TABLE IV. Calculated values of the adsorption energy E_{ad}, binding energy of hydrogen E_b, adsorption height h_0, top-layer relaxation Δd_{12}, and work-function change $\Delta\Phi$ for H on Rh(100). For the clean surface the top-layer relaxation is −3.5% and the work function is 5.25 eV.

Adsorption site	Coverage Θ	E_b [eV]	E_{ad} [eV]	h_0 [Å]	Δd_{12} $\%d_0$	$\Delta\Phi$ [meV]
Hollow	1	2.79	0.42	0.38	+1.1	+390
Bridge	1	2.62	0.24	1.15	−0.6	+490
Subsurface (O_h)	1	2.11	−0.26		+5.4	−30

tion change of 390 meV is found. This is in agreement with measurements at field emission microscope tips.[52] In the case, that one bridge site per surface Rh atom is occupied, the work function increases by 490 meV. It is interesting to note that similar to Pd(100), a decrease of the work function of −500 meV in comparison to the clean surface is obtained if both bridge sites ($\Theta = 2$) become occupied. The small and even decreasing work function found in the coverage regime between $\Theta = 0.5$ and $\Theta = 1$ in Ref. 51 may be attributed to a partial occupation of such double bridge configurations.

IV. CONCLUSION

In conclusion, we calculated the adsorption energy, the equilibrium geometries, and the changes in work function for hydrogen adsorption at Pd(100) and Rh(100) in dependence of hydrogen coverage.

Up to monolayer coverage hydrogen occupies the fourfold surface hollow sites at both the Pd(100) and the Rh(100) surface in agreement with experiment. The adsorption energy is similar at both surface (≈ 0.5 eV) and nearly independent of coverage. In the case of Pd(100) hydrogen placed at octahedral subsurface sites has a large adsorption energy. In contrast, subsurface (O_h) sites are found to be unfavorable at Rh(100) in correspondence with the instability of bulk RhH.

At coverages $\Theta > 1$ hydrogen occupies subsurface (O_h) positions at Pd(100) in addition to the fully occupied surface hollow sites. This is the main result of our paper. In accordance with experiment the differential adsorption energy strongly decreases after monolayer coverage and is expected to saturate close to the value found for the subsurface sites if it would be possible to occupy the subsurface layer with larger hydrogen concentrations. Configurations where in addition to the surface hollow site a second surface adsorption site is occupied are energetically unfavorable at Pd(100).

The work function increases if hydrogen adsorbs at the Pd(100) and Rh(100) surface due to an accumulation of screening charge in the surface region. For coverages $\Theta > 1$ of hydrogen at the Pd(100) surface, i.e., in the case that subsurface (O_h) sites become occupied the work function remains nearly at the $\Theta = 1$ level. A deviation from this trend is possible at small concentrations of hydrogen in subsurface positions.

The picture of hydrogen adsorption on Pd(100) developed in this paper gives consistent interpretation of experimental data.[3,6,8,9] Different explanations of the second regime of hydrogen adsorption observed in Ref. 3 as, e.g., the presence of other types of adsorbates[17] cannot be excluded at present. Further experimental work studying subsurface occupations of hydrogen at Pd(100) is highly desirable.

ACKNOWLEDGMENTS

The critical and stimulating discussions with M. Scheffler and M. Methfessel are gratefully acknowledged.

[1] K. Christmann, Surf. Sci. Rep. **9**, 1 (1988).
[2] R. Duš, Surf. Sci. **42**, 324 (1973).
[3] R. J. Behm, K. Christmann, and G. Ertl, Surf. Sci. **99**, 320 (1980).
[4] Y. Kim, H. C. Peebles, and J. M. White, Surf. Sci. **114**, 363 (1982).
[5] D. G. Castner, B. A. Sexton, and G. A. Somorjai, Surf. Sci. **71**, 519 (1978).
[6] C. Nyberg and C.G. Tengstål, Solid State Commun. **44**, 251 (1982); Phys. Rev. Lett. **50**, 1680 (1983); Surf. Sci. **126**, 163 (1983).
[7] L. J. Richter and W. Ho, J. Vac. Sci. Technol. A**5**, 453 (1986).
[8] F. Besenbacher, I. Stensgaard, and K. Mortensen, Surf. Sci. **191**, 288 (1987).
[9] K. H. Rieder and W. Stocker, Surf. Sci. **110**, 139 (1984).
[10] E. Wicke and H. Brodowsky, in *Hydrogen in Metals*, edited by G. Alefeld and J. Völkl (Springer, Berlin, 1978), Vol. 2, p. 73.
[11] R. J. Behm, Ph.D. thesis, Ludwig-Maximilians-Universität München, Germany, 1980.
[12] R. F. Willis and E. W. Plummer, Surf. Sci. **80**, 593 (1979).
[13] G. E. Gdowski, T. E. Felter, and R. H. Stulen, Surf. Sci. **181**, L147 (1986).
[14] T. E. Felter, E. C. Sowa, and M. A. Van Hove, Phys. Rev. B **40**, 891 (1989).
[15] K. H. Rieder, M. Baumberger, and W. Stocker, Phys. Rev. Lett. **51**, 1799 (1983).
[16] M. Skottke, R. J. Behm, and G. Ertl, J. Chem. Phys. **87**, 6191 (1987).
[17] M. L. Burke and R. J. Madix, Surf. Sci. **237**, 1 (1990).
[18] V. E. Antonov, I. T. Belash, V. F. Degtyareva, and E. G. Ponyativskii, Dokl. Akad. Nauk SSSR **239**, 342 (1978) [Sov. Phys. Dokl. **238/240**, 222 (1978)]; R. B. McLellan and W. A. Oates, Acta Metall. **21**, 181 (1973).
[19] D. Tománek, S. G. Louie, and Che-Ting Chan, Phys. Rev. Lett. **57**, 2594 (1986).
[20] D. Tománek, Z. Sun, and S. G. Louie, Phys. Rev. B **43**, 4699 (1991).
[21] C. T. Chan and S. G. Louie, Phys. Rev. B **30**, 4153 (1984).
[22] D. R. Hamann and P. J. Feibelman, Phys. Rev. B **37**, 3847 (1988).
[23] P. J. Feibelman and D. R. Hamann, Surf. Sci. **234**, 377 (1990).
[24] P. J. Feibelman, Phys. Rev. B **43**, 9452 (1991).
[25] P. J. Feibelman, Phys. Rev. Lett. **67**, 461 (1991).
[26] M. Methfessel, Phys. Rev. B **38**, 1537 (1988); M. Methfessel, C. O. Rodriguez, and O. K. Andersen, *ibid.* **40**, 2009 (1989).
[27] M. Methfessel, D. Hennig, and M. Scheffler, Phys. Rev. B **46**, 4816 (1992).
[28] D. Hennig, S. Wilke, R. Löber, and M. Methfessel, Surf. Sci. **287/288**, 89 (1993).
[29] S. Wilke, D. Hennig, R. Löber, M. Methfessel, and M. Scheffler, Surf. Sci. **307-309**, 76 (1994).
[30] J. P. Perdew and A. Zunger, Phys. Rev. B **23**, 5048 (1981).
[31] R. S. Mulliken, J. Chem. Phys. **23**, 1833 (1955); **23**, 1841 (1955).

[32] R. Hoffmann, Rev. Mod. Phys. **60**, 601 (1988).
[33] M. H. Cohen, M. V. Ganduglia-Pirovano, and J. Kudrnovský, Phys. Rev. Lett. **72**, 3222 (1994).
[34] K. Christmann, *Introduction to Surface Physical Chemistry* (Steinkopf Verlag, Darmstadt, 1991), pp. 11ff.
[35] K. P. Huber and G. Herzberg, *Molecular Structure and Molecular Spectra. IV. Constants of Diatomic Molecules* (Van Nostrand Reinhold, New York, 1979).
[36] C. Kittel, *Introduction to Solid State Physics*, 5th ed. (Wiley, New York, 1976), p. 85.
[37] J. Hölzl and F. K. Schulte, *Solid Surface Physics*, Springer Tracts in Modern Physics, Vol. 85 (Springer Verlag, Berlin, 1979), p. 1.
[38] P. Nordlander, S. Holloway, and J. K. Nørskov, Surf. Sci. **136**, 59 (1984).
[39] P. J. Feibelman and D. R. Hamann, Surf. Sci. **179**, 153 (1987).
[40] W. Zhong, Y. Cai, and D. Tománek, Phys. Rev. B **46**, 8099 (1992).
[41] J. Quinn, Y. S. Li, D. Tian, F. Jona, and P. M. Marcus, Phys. Rev. B **42**, 11 348 (1990).
[42] L. Stauffer, R. Riedinger, and H. Dreyssé, Surf. Sci. **238**, 83 (1990).
[43] T. L. Einstein, M. S. Daw, and S. M. Foiles, Surf. Sci. **227**, 114 (1990).
[44] W. Eberhardt, S. G. Louie, and E. W. Plummer, Phys. Rev. B **28**, 465 (1983).
[45] W. Eberhardt, F. Greuter, and E. W. Plummer, Phys. Rev. Lett. **46**, 1085 (1981).
[46] S. G. Louie, Phys. Rev. Lett. **42**, 476 (1979).
[47] P. J. Feibelman and D. R. Hamann, Phys. Rev. Lett. **52**, 61 (1984).
[48] P. Nordlander and S. Holmström, Surf. Sci. **159**, 443 (1985).
[49] C. Elsässer, M. Fähnle, K. M. Ho, and C. T. Chan, Physica B **172**, 217 (1991).
[50] C. Elsässer, K. M. Ho, C. T. Chan, and M. Fähnle, J. Phys. CM**4**, 5207 (1992).
[51] D. E. Peebles, H. C. Peebles, and J. M. White, Surf. Sci. **136**, 463 (1984).
[52] V. V. Gorodetskii, B. E. Nieuwenhuys, W. H. H. Sachtler, and G. K. Boreskov, Surf. Sci. **108**, 225 (1981).

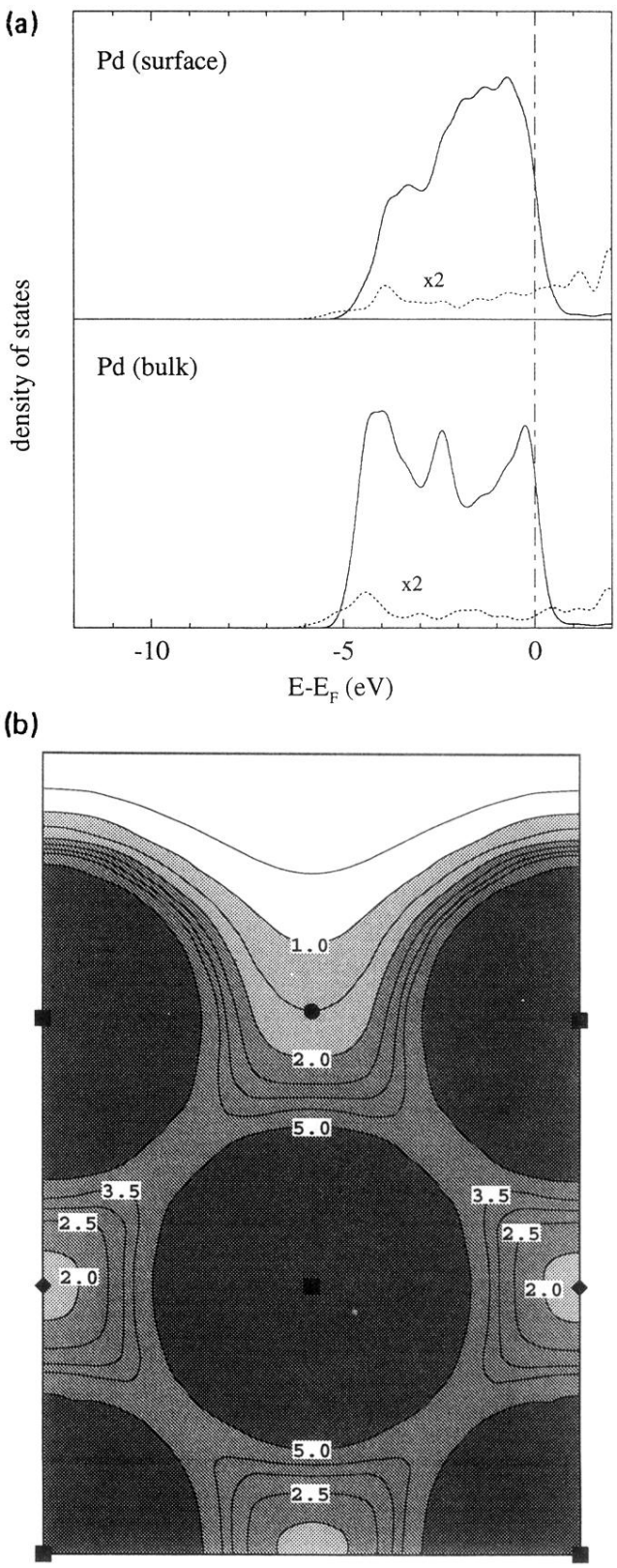

FIG. 1. Layer and symmetry resolved DOS (a) and charge density distribution (b) at the clean Pd(100) surface. (a) DOS projected to the d (solid line) and s,p functions (dashed line) of the surface (upper panel) and bulk (lower panel) Pd atoms. (b) Charge density for a cut plane perpendicular to the surface and along the $\langle 100 \rangle$ direction. The scale is given in 10^{-2} bohr^{-3}.

(a)

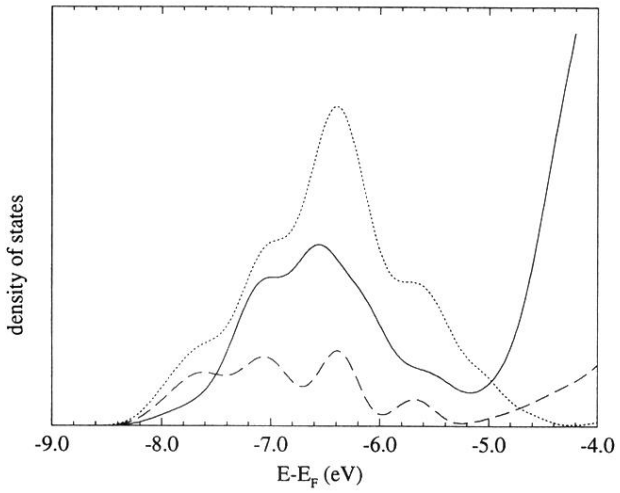

(b)

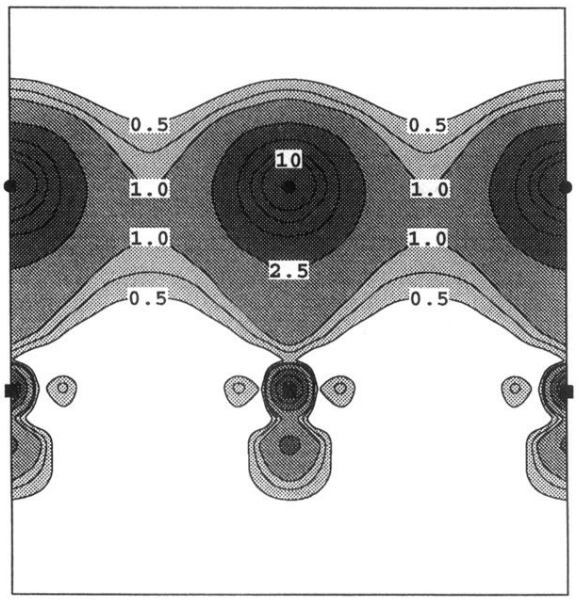

FIG. 4. Layer and symmetry resolved DOS (a) and charge density distribution (b) in the energy range of the split-off band of the Pd(100)-(1×1)-H(hollow) structure. (a) DOS projected to hydrogen s, p functions (dashed-dotted line) and to the d (solid line) and s, p functions (dashed line) of the surface Pd atoms. (b) Charge density for a cut plane perpendicular to the surface and along the $\langle 110 \rangle$ direction. The scale is given in 10^{-2} bohr^{-3}.

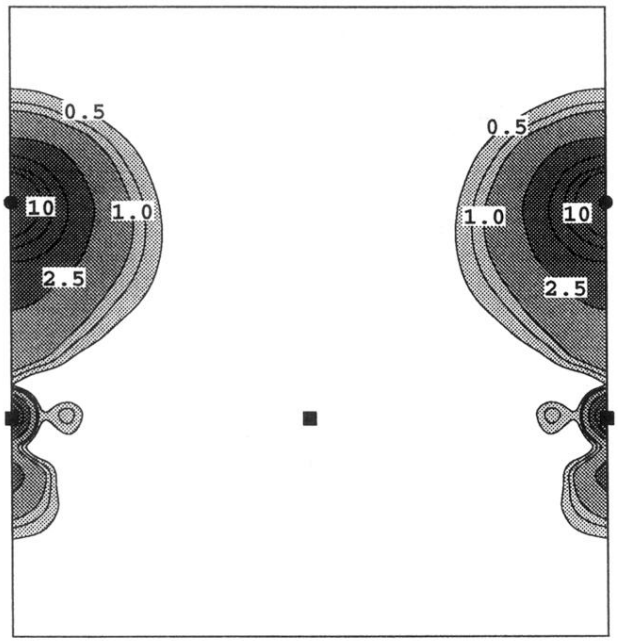

FIG. 5. Charge density distribution in the energy range of the split-off band of the Pd(100)-(2×2)-H (hollow) structure in the same cut plane as in Fig. 4.

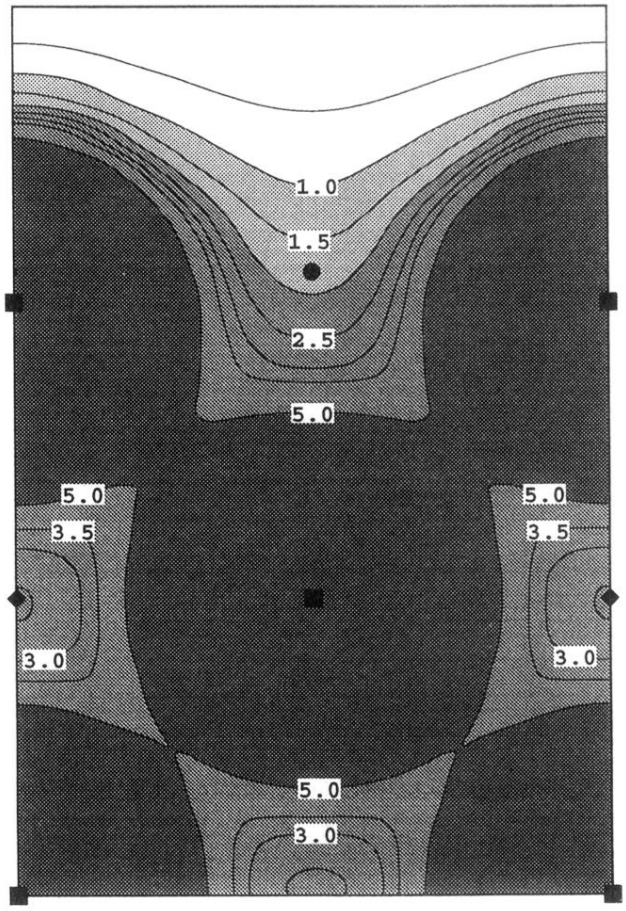

FIG. 7. Charge density distribution at the clean Rh(100) surface for the same cut plane as in Fig. 1.